

## THE DETAILED OPTICAL LIGHT CURVE OF GRB 030329

Y. M. LIPKIN,<sup>1,2</sup> E. O. OFEK,<sup>1,2</sup> A. GAL-YAM,<sup>1,2</sup> E. M. LEIBOWITZ,<sup>1</sup> D. POZNANSKI,<sup>1</sup> S. KASPI,<sup>1</sup> D. POLISHOOK,<sup>1</sup> S. R. KULKARNI,<sup>3</sup>  
D. W. FOX,<sup>3</sup> E. BERGER,<sup>3</sup> N. MIRABAL,<sup>4</sup> J. HALPERN,<sup>4</sup> M. BUREAU,<sup>4</sup> K. FATHI,<sup>5,6</sup> P. A. PRICE,<sup>7</sup> B. A. PETERSON,<sup>7</sup>  
A. FREBEL,<sup>7</sup> B. SCHMIDT,<sup>7</sup> J. A. OROSZ,<sup>8</sup> J. B. FITZGERALD,<sup>8</sup> J. S. BLOOM,<sup>9</sup> P. G. VAN DOKKUM,<sup>10</sup>  
C. D. BAILYN,<sup>10</sup> M. M. BUXTON,<sup>10</sup> AND M. BARSONY<sup>11,12</sup>

Received 2003 December 7; accepted 2004 January 19

### ABSTRACT

We present densely sampled *BVR*I light curves of the optical transient associated with the gamma-ray burst (GRB) 030329, the result of a coordinated observing campaign conducted at five observatories. Augmented with published observations of this GRB, the compiled optical data set contains 2687 photometric measurements, obtained between 78 minutes and 79 days after the burst. This data set allows us to follow the photometric evolution of the transient with unprecedented detail. We use the data to constrain the light curve of the underlying supernova (SN) 2003dh and show that it evolved faster than and was probably somewhat fainter than the Type Ic SN 1998bw, associated with GRB 980425. We find that our data can be described by a broken power-law decay perturbed by a complex variable component. The early- and late-time decay slopes are determined to be  $\alpha_1 \approx 1.1$  and  $\alpha_2 \approx 2$ . Assuming this single-break power-law model, we constrain the break to lie between  $\sim 3$  and  $\sim 8$  days after the burst. This simple, singly broken power-law model, derived only from the analysis of our optical observations, may also account for available multiband data, provided that the break happened  $\sim 8$  days after the burst. The more complex double-jet model of Berger et al. provides a comparable fit to the optical, X-ray, millimeter, and radio observations of this event. The unique early coverage available for this event allows us to trace the color evolution of the afterglow during the first hours after the burst. We detect a significant change in optical colors during the first day. Our color analysis is consistent with a cooling-break frequency sweeping through the optical band during the first day. The light curves of GRB 030329 reveal a rich array of variations, superposed over the mean power-law decay. We find that the early variations ( $\lesssim 8$  days after the burst) are asymmetric, with a steep rise followed by a relatively slower (by a factor of about 2) decline. The variations maintain a similar timescale during the first 4 days and then get significantly longer. The structure of these variations is similar to those previously detected in the afterglows of several GRBs.

*Subject headings:* gamma rays: bursts — supernovae: general — supernovae: individual (SN 2003dh)

*On-line material:* machine-readable table

### 1. INTRODUCTION

Following the discovery of low-energy transients associated with long-duration ( $>2$  s) gamma-ray bursts (GRBs; van Paradijs et al. 1997), a major effort was made to characterize the temporal evolution of these sources across the

electromagnetic spectrum. In the optical regime, the associated transient sources were found to decline rapidly with time. The emission from the first optical transients (OTs) discovered was reported to decay as a power law with time, extending from the epoch of discovery and continuing for tens of days (e.g., GRB 970228, Galama et al. 1997; GRB 970508, Galama et al. 1998a; Sokolov et al. 1998; Bloom et al. 1998).

The decay slopes measured for OTs were used to constrain explosion models. In particular, with the increasing popularity of nonisotropic models (involving highly relativistic jets or cones), a temporal break in the decline slope was predicted (e.g., Rhoads 1997; Panaitescu, Mészáros, & Rees 1998; Sari, Piran & Halpern 1999) and detected (e.g., Castro-Tirado et al. 1999; Kulkarni et al. 1999; Stanek et al. 1999; Harrison et al. 1999; Price et al. 2001).

Following the discovery of supernova (SN) 1998bw in the error box of GRB 980425 (Galama et al. 1998b), the association of GRBs with SN explosions came into focus. Late-time “bumps” in OT light curves were interpreted as the signature of underlying SN explosions (e.g., Bloom et al. 1999). While observational evidence supporting the SN hypothesis accumulated (e.g., Bloom et al. 2002; Garnavich et al. 2003b; Price et al. 2003a), a direct observational proof for the existence of an underlying SN explosion has long remained missing, and alternative explanations for the origin of these bumps were suggested (e.g., Waxman & Draine 2000; Esin & Blandford 2000; Reichart 2001).

<sup>1</sup> School of Physics and Astronomy and Wise Observatory, Tel-Aviv University, Tel-Aviv 69978, Israel; yiftah@wise.tau.ac.il, eran@wise.tau.ac.il, avishay@wise.tau.ac.il.

<sup>2</sup> The first three authors contributed equally to this work.

<sup>3</sup> Division of Physics, Mathematics and Astronomy, 105-24, California Institute of Technology, 1200 East California Boulevard, Pasadena, CA 91125.

<sup>4</sup> Columbia Astrophysics Laboratory, Columbia University, 550 West 120th Street, New York, NY 10027.

<sup>5</sup> School of Physics and Astronomy, University of Nottingham, Nottingham NG7 2RD, UK.

<sup>6</sup> Kapteyn Astronomical Institute, P.O. Box 800, 9700 AV Groningen, Netherlands.

<sup>7</sup> Research School of Astronomy and Astrophysics, Australian National University, Mt. Stromlo Observatory, Weston Creek P.O., ACT 2611, Australia.

<sup>8</sup> Department of Astronomy, San Diego State University, 5500 Campanile Drive, San Diego, CA 92182.

<sup>9</sup> Harvard Society of Fellows, 78 Mount Auburn Street, Cambridge, MA 02138; and Harvard-Smithsonian Center for Astrophysics, MC 20, 60 Garden Street, Cambridge, MA 02138.

<sup>10</sup> Department of Astronomy, Yale University, New Haven, CT 06520-8101.

<sup>11</sup> Department of Physics and Astronomy, San Francisco State University, 1600 Holloway Avenue, San Francisco, CA 94132-4163.

<sup>12</sup> Space Science Institute, 3100 Marine Street, Suite A353, Boulder, CO 80303-1058.

With growing interest and efforts by the astronomical community, the observed OT light curves became increasingly better measured. In particular, for some OTs, a dense temporal sampling of the light curve, sometimes starting shortly (minutes to hours) after the GRB trigger, was carried out by worldwide observing networks. A case to note is the OT of GRB 021004, where multiple bumps and wiggles in the light curve, probably not associated with an SN, were first observed (e.g., Bersier et al. 2003; Mirabal et al. 2003; Fox et al. 2003).

On 2003 March 29, a bright GRB was detected by the *HETE-2* spacecraft (Vanderspek et al. 2003). The early discovery of the associated OT (Peterson & Price 2003; Torii 2003; Torii et al. 2003; Price et al. 2003b; Uemura et al. 2003; Sato et al. 2003), and its brightness, triggered a worldwide observational effort involving tens of ground- and space-based facilities observing in various wavelengths, from X-ray to radio. The brightness of the OT allowed the prompt determination of the redshift of the source. At  $z = 0.1685$  (Greiner et al. 2003a), this event is the closest GRB to date for which a typical OT has been discovered. The relatively low redshift of this burst presented a unique opportunity to search for a clear spectroscopic signature of an underlying SN. Indeed, intensive spectroscopic monitoring of the optical source revealed the emerging spectrum of a Type Ic SN 1998bw-like event, designated SN 2003dh, conclusively proving that at least some of the long-duration GRBs are associated with SN explosions (Stanek et al. 2003; Hjorth et al. 2003; Matheson et al. 2003).

Numerous works have already presented observations of this unique event. Early optical observations, obtained with small telescopes shortly after the burst, were reported by Uemura et al. (2003), Torii et al. (2003), Smith et al. (2003), Sato et al. (2003), and Urata et al. (2004). Burenin et al. (2003), Bloom et al. (2004), and Matheson et al. (2003) presented the results of multiband follow-up campaigns in the optical and near-IR. Greiner et al. (2003b) presented optical polarization monitoring of GRB 030329, detecting significant variability. These works mostly relied on data collected at a single geographical location, thus limiting their ability to achieve a continuous temporal coverage. Intensive monitoring of the afterglow of GRB 030329 in the radio and millimeter wavelengths was reported by Berger et al. (2003) and Sheth et al. (2003), while X-ray observations were reported by Tiengo et al. (2003).

In this paper, we report the results of an intensive, coordinated, worldwide campaign designed to follow the light curve of the OT associated with GRB 030329. Combining data from five observatories in three continents, we achieved an almost continuous coverage of the OT during the first few days after the GRB. Careful cross-calibration was used to bring data collected by using many different instruments to the same reference system. This internally consistent data set has allowed us to correctly incorporate four other sets of observations now available in the literature. The final light curves that we compiled are unprecedented in their temporal sampling and reveal a uniquely rich and complicated photometric evolution. We assume throughout a cosmology with  $\Omega_m = 0.3$ ,  $\Omega_\Lambda = 0.7$ , and  $H_0 = 65 \text{ km s}^{-1} \text{ Mpc}^{-1}$ .

## 2. OBSERVATIONS AND DATA REDUCTION

We performed time-resolved CCD photometry of the OT at five observatories from March 29.72 to June 17.19 UT (from 5.66 hr to 79.7 days after the burst). Observations were

carried out through *B*, *V*, *R*, and *I* filters, accumulating a total of 77, 104, 928, and 96 data points, respectively. Details of the equipment and a summary of the observations are given in Table 1.

The images were bias-subtracted and flat-field-corrected in the standard fashion. In each frame we measured the magnitude of the OT, as well as of several reference stars, with an aperture of  $2''$  radius. Three to nine reference stars were measured in each subset, depending on the depth and the field of view of the images. All of the reference stars were tested to be nonvariable. The reference stars used in each subset are listed in Table 2.

For each of the detectors used, we obtained a set of internally consistent magnitudes of the OT by minimizing the scatter of the reference stars over the subset. Outlying measurements were removed during the process. Apparently underestimated errors in the photometry of reference stars were increased so that  $\chi^2/\text{dof} = 1$  (where dof is the number of degrees of freedom) for each of the reference stars in the subset.

Cross-calibration including color terms of the different instruments was carried out by transforming the photometric system of each of the subsets to the one of Henden (2003). The transformation parameters were derived by linearly fitting the differences between the weighted-mean magnitude of the reference stars and their magnitudes in the Henden (2003) system to the colors of the reference stars reported by this author. Because of the initial uncertainty in the OT colors, two iterations were required to transform its magnitudes to the reference system. The transformation uncertainty of each data subset was added in quadrature to the measured photometric errors. The photometric errors do not include the uncertainty in the zero point of the calibration, 0.02 mag (Henden 2003).

The photometric measurements obtained at the Mount Laguna Observatory failed to yield consistent color terms and were therefore cross-calibrated by eliminating the offset between overlapping segments of this subset and the rest of the light curve. From the residual scatter in these overlapping segments, we estimate the resultant systematic cross-calibration errors of this set to be  $\sim 5\%$ .

We augmented our data set with external photometry from Burenin et al. (2003), Uemura et al. (2003), and Bloom et al. (2004), kindly provided in digital form by these authors, as well as with the data published by Matheson et al. (2003). Each of the external data sources was cross-calibrated with our set by using the procedure described above for the Mount Laguna Observatory data. Since the color of the OT changed with time, this process may have introduced small systematic errors. From the scatter between the external sets and our light curves, we estimate this error to be smaller than 5%.

A few data segments from Uemura et al. (2003), temporally overlapping with our own, were not incorporated into our light curve because the photometric errors in these segments (and hence the scatter of the data points) were greater than in our data. We note, however, that our data and those of Uemura et al. are in good agreement throughout the overlapping segments. The *I*-band light curve of Burenin et al. (2003), covering the time span between 0.2 and 0.6 days, does not overlap with our *I*-band data. The zero point for this segment was set by coarsely extrapolating later *I*-band segments and should therefore be regarded with caution.

The earliest available observations of the OT ( $\sim 1.3$  hr after the burst) were obtained by two groups. A set of unfiltered observations were reported by Uemura et al. (2003), who

TABLE 1  
LIST OF OBSERVATORIES

| ID                                          | Observatory+Instrument | East Longitude<br>(deg) | Filter (Number of Observations)                                |
|---------------------------------------------|------------------------|-------------------------|----------------------------------------------------------------|
| Observatories Participating in Our Campaign |                        |                         |                                                                |
| 01.....                                     | Wise 1 m+Tek           | 34.8                    | <i>B</i> (9), <i>V</i> (25), <i>R</i> (484), <i>I</i> (25)     |
| 02.....                                     | Wise 1 m+SITe          | 34.8                    | <i>B</i> (8), <i>V</i> (7), <i>R</i> (57)                      |
| 03.....                                     | SSO 1 m+WFI            | 149.1                   | <i>B</i> (5), <i>V</i> (2), <i>R</i> (5), <i>I</i> (2)         |
| 05.....                                     | MDM 1.3 m+2.4 m+SITe   | -111.6                  | <i>B</i> (1), <i>V</i> (1), <i>R</i> (311), <i>I</i> (1)       |
| 06.....                                     | Palomar 1.5 m+Norris   | -116.9                  | <i>I</i> (3)                                                   |
| 07.....                                     | Mt. Laguna 1 m+Loral   | -116.4                  | <i>B</i> (54), <i>V</i> (69), <i>R</i> (71), <i>I</i> (67)     |
| External Data Sources                       |                        |                         |                                                                |
| 21.....                                     | Kyoto <sup>a</sup>     | ~135                    | CR (391) <sup>b</sup>                                          |
| 31.....                                     | RTT <sup>c</sup>       | 30.3                    | <i>B</i> (144), <i>V</i> (167), <i>R</i> (168), <i>I</i> (165) |
| 41.....                                     | CTIO 1.3 <sup>d</sup>  | -70.8                   | <i>B</i> (9), <i>V</i> (13), <i>I</i> (13)                     |
| 51.....                                     | FLWO <sup>e</sup>      | -110.9                  | <i>B</i> (62), <i>V</i> (57), <i>R</i> (111), <i>I</i> (57)    |
| 52.....                                     | KAIT <sup>e</sup>      | -121.6                  | <i>B</i> (14), <i>V</i> (15), <i>R</i> (15), <i>I</i> (15)     |
| 53.....                                     | LCO <sup>e</sup>       | -70.7                   | <i>B</i> (4), <i>V</i> (4), <i>I</i> (4)                       |
| 54.....                                     | LCO-40 <sup>e</sup>    | -70.7                   | <i>R</i> (2)                                                   |
| 55.....                                     | KPNO 4 m <sup>c</sup>  | -111.6                  | <i>B</i> (19), <i>R</i> (4)                                    |
| 56.....                                     | Magellan2 <sup>e</sup> | -70.7                   | <i>R</i> (25)                                                  |
| 57.....                                     | Dupont <sup>e</sup>    | -70.7                   | <i>B</i> (4)                                                   |

<sup>a</sup> Several observatories in Japan; Uemura et al. 2003.

<sup>b</sup> Unfiltered observations transformed to *R* band; see Uemura et al. 2003.

<sup>c</sup> Burenin et al. 2003.

<sup>d</sup> Bloom et al. 2004.

<sup>e</sup> Matheson et al. 2003.

transformed the resulting magnitudes to the standard *R* band. After cross-calibration, these data are in good agreement with the rest of our data. A couple of measurements in standard *R* were taken through clouds with the Siding Spring Observatory (SSO) 1 m telescope (Price et al. 2003b). After cross-calibration, the two points yielded significantly brighter measurements, by about 0.1 mag. Other observations from the SSO 1 m telescope, taken under better conditions, are in good agreement with the rest of the data. Because of the good

agreement between the bulk of our data and those of Uemura et al. (2003) and because of the unfavorable weather conditions under which the early SSO images were obtained, we preferred the light curve of the former over the latter two points. The results we present below, however, are insensitive to this selection and would remain essentially the same had we corrected the data of Uemura et al. to fit the SSO points. The recently reported early observations by Torii et al. (2003) are even brighter than the SSO points. Thus, it appears that

TABLE 2  
REFERENCE STARS

| Coordinates (2000)            | Number <sup>a</sup> | <i>V</i> Magnitude <sup>a</sup><br>(mag) | Used in Sets <sup>b</sup> |
|-------------------------------|---------------------|------------------------------------------|---------------------------|
| 10 44 28.62, +21 27 45.4..... | 005                 | 15.587                                   | 2, 3, 6                   |
| 10 44 36.86, +21 26 59.1..... | 016                 | 13.266                                   | 6                         |
| 10 44 39.07, +21 30 59.1..... | 019                 | 17.616                                   | 1, 3, 6, 7                |
| 10 44 39.86, +21 34 15.0..... | 021                 | 16.842                                   | 1, 3, 6                   |
| 10 44 41.75, +21 31 52.6..... | 026                 | 19.331                                   | 3, 5, 7                   |
| 10 44 42.02, +21 32 32.1..... | 027                 | 16.839                                   | 2, 3, 5, 7                |
| 10 44 48.03, +21 34 18.5..... | 037                 | 17.909                                   | 1, 2, 3                   |
| 10 44 53.66, +21 30 12.1..... | 047                 | 18.396                                   | 6                         |
| 10 44 54.45, +21 34 29.2..... | 049                 | 14.136                                   | 3                         |
| 10 44 54.99, +21 29 46.3..... |                     | 20.275 <sup>c</sup>                      | 5                         |
| 10 44 55.00, +21 31 42.9..... | 050                 | 19.598                                   | 7                         |
| 10 45 06.48, +21 36 13.7..... | 093                 | 16.245                                   | 2                         |
| 10 45 09.81, +21 35 10.2..... | 098                 | 15.469                                   | 2,3                       |
| 10 45 15.36, +21 34 16.1..... | 110                 | 14.730                                   | 2, 3, 6                   |

NOTE.—Units of right ascension are hours, minutes, and seconds, and units of declination are degrees, arcminutes, and arcseconds.

<sup>a</sup> Star numbers and magnitudes refer to the photometry of Henden 2003.

<sup>b</sup> Observatory IDs given in Table 1.

<sup>c</sup> Photometry measured in our data set and scaled to the system of Henden 2003.

TABLE 3  
OBSERVATIONS

| Observatory<br>Code<br>(1) | Filter<br>(2) | MJD<br>(3) | $t$<br>(days)<br>(4) | Magnitude<br>(mag)<br>(5) | $e_{\text{mag}}$<br>(mag)<br>(6) | $E_{\text{mag}}$<br>(mag)<br>(7) |
|----------------------------|---------------|------------|----------------------|---------------------------|----------------------------------|----------------------------------|
| 01.....                    | 04            | 2729.21443 | 1.23024              | 16.438                    | 0.018                            | 0.050                            |
| 01.....                    | 04            | 2729.21597 | 1.23177              | 16.414                    | 0.020                            | 0.051                            |
| 01.....                    | 04            | 2729.21749 | 1.23329              | 16.447                    | 0.018                            | 0.050                            |
| 01.....                    | 04            | 2729.21900 | 1.23481              | 16.398                    | 0.019                            | 0.050                            |
| 01.....                    | 04            | 2729.22052 | 1.23632              | 16.415                    | 0.018                            | 0.050                            |
| 01.....                    | 04            | 2729.22203 | 1.23783              | 16.432                    | 0.018                            | 0.050                            |
| 01.....                    | 04            | 2729.22355 | 1.23936              | 16.434                    | 0.018                            | 0.050                            |
| 01.....                    | 03            | 2729.22956 | 1.24536              | 16.786                    | 0.012                            | 0.022                            |
| 01.....                    | 05            | 2729.23286 | 1.24866              | 15.940                    | 0.011                            | 0.060                            |
| 01.....                    | 04            | 2729.23549 | 1.25129              | 16.416                    | 0.013                            | 0.048                            |

NOTES.—Table 3 is published in its entirety in the electronic edition of the *Astrophysical Journal*. A portion is shown here for guidance regarding its form and content. The data are also available from our Web site, <http://wise-obs.tau.ac.il/GRB030329>. Col. (1): the observatory code (see Table 1); col. (2): the filter used; 02, 03, 04, and 05 are for  $B$ ,  $V$ ,  $R$ , and  $I$ , respectively; col. (3):  $\text{JD} - 2,450,000$ ; col. (4): time since  $t_{\text{burst}} = 2,452,727.98419757$ ; col. (5): calibrated magnitude; col. (6): the error in magnitude including the self-calibration error of the individual observatory; col. (7): the error in magnitude including the uncertainty in cross-calibrating the various observatories.

forming a consistent picture of the early light curve of this event will require further analysis, once all the relevant data are available.

Altogether, we compiled 2687 photometric measurements (333, 360, 1644, and 350 in  $B$ ,  $V$ ,  $R$ , and  $I$ , respectively), making GRB 030329 the most extensively studied extragalactic cosmic explosion in the optical regime, with the possible exception of SN 1987A. The complete set of photometric measurements presented in this paper are listed in Table 3.

### 3. THE LIGHT CURVE

The final  $BVR$ I light curves of GRB 030329 are presented in Figure 1. Our best-sampled set is the  $R$ -band light curve, with an almost continuous coverage during  $0.05 \text{ days} \lesssim t \lesssim 3 \text{ days}$  and a relatively dense sampling up to  $t \approx 67 \text{ days}$ .

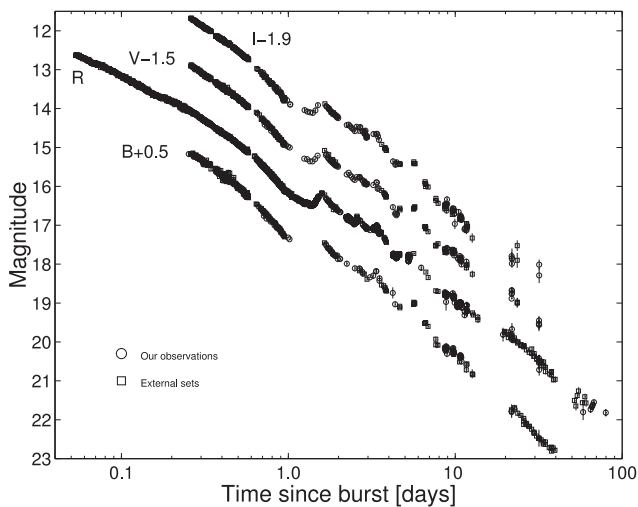


FIG. 1.— $BVR$ I light curve of GRB 030329. Our observations are marked by circles, and the external data sets (see Table 1), cross-calibrated to our photometric system, are marked by squares. For presentation purposes the  $BVR$ I light curves are shifted vertically by +0.5,  $-1.5$ , and  $-1.9 \text{ mag}$ , respectively.

We therefore focus our attention on this light curve and augment our analysis with results from other bands when necessary.

While the OT grossly follows a power-law declining trend, it shows remarkably strong short-term deviations from the smooth, monotonic decline, particularly in the range  $0.05 \text{ days} \lesssim t \lesssim 5 \text{ days}$ . Later periods, in the range  $8 \text{ days} \lesssim t \lesssim 14 \text{ days}$  and at  $t \gtrsim 50 \text{ days}$ , also feature pronounced variations of the light curve. We note that the light curves do not show a priori any clear distinction between “early” and “late” power-law components—the signature of a break in the decline rate. We also note the lack of a clear bump that may be attributed to SN 2003dh, although its significant contribution to the total brightness of the OT was established spectroscopically.

At  $R = 23.25 \pm 0.15 \text{ mag}$  (A. S. Fruchter 2003, private communication), the host becomes a significant contributor to the observed flux during the late decline phase of the OT. Hence, below, unless stated otherwise, we discuss the  $R$ -band light curve of the OT only, obtained by subtracting the host flux from our measurements. The photometric errors of the OT were modified to include the uncertainty in the host galaxy magnitude.

To further discuss the light curve, we decompose it into an SN component and an “afterglow” component, which is further divided into two components: a smooth, monotonic decline component (the main observational characteristic of GRB afterglows) and a perturbation component—variations over different timescales and intensities about the smooth decay of GRB 030329. In the following sections we consider each of the OT components separately.

#### 3.1. The Supernova Component

Spectroscopic analysis of SN 2003dh (Stanek et al. 2003; Hjorth et al. 2003; Matheson et al. 2003; Chornock et al. 2003) revealed a remarkable similarity to the well-studied SN 1998bw associated with GRB 980425 (although see Mazzali et al. 2003; Kawabata et al. 2003). In light of this similarity, we base our investigation of the SN component in the afterglow of GRB 030329 on the known properties of SN 1998bw.

We constrain the SN component by comparing the OT light curve with four alternative models for SN 2003dh. All four models are modifications of the light curve of SN 1998bw, corrected to the redshift of SN 2003dh ( $z = 0.1685$ ). The transformation was carried out by applying synthetic photometry (using the methods presented in Poznanski et al. 2002) to the large collection of SN 1998bw spectra reported by Patat et al. (2001) and taking into account the greater luminosity distance of SN 2003dh (810 Mpc, compared with 37 Mpc for SN 1998bw), cosmological redshift, and time dilation effects, as well as the shift in the SN spectrum sampled by each filter ( $K$ -corrections). The SN light curve was also corrected for Galactic extinction in the direction of SN 2003dh ( $E_{B-V} = 0.025$  mag; Schlegel, Finkbeiner, & Davis 1998) but was not corrected for the host galaxy extinction (see below). Our derived light curves are in good agreement with those computed by Bloom et al. (2004) using a slightly different approach.

Comparing the models with the data, we note that any variation in the light curve should probably be attributed to the afterglow, since no such variations have been detected in the light curves of any of the well-observed SNe Ic (e.g., SN 1998bw, Galama et al. 1998b; McKenzie & Schaefer 1999; Patat et al. 2001; SN 2002ap, Gal-Yam, Ofek, & Shemmer 2002; Pandey et al. 2003; Yoshii et al. 2003; Foley et al. 2003; SN 1999ex, Stritzinger et al. 2002; SN 1994I, Yokoo et al. 1994). A valid SN model is therefore required to be fainter than the bottom of the dips in the light curve. In particular, the minima of two rebrightening episodes in the  $R$  band, one of  $\sim 0.3$  mag around  $t \approx 52$  days and another of  $\sim 0.2$  mag around  $t \approx 68$  days (see § 3.3), set upper limits on the SN magnitude of  $R = 21.93 \pm 0.15$  and  $22.04 \pm 0.13$  mag, respectively, at the times of these episodes.

Figure 2 shows the  $R$ -band light curve of the OT (*open circles*). Overlaid are the four different model light curves for the SN component. The solid line in Figure 2 is the redshift-corrected light curve of SN 1998bw described above,

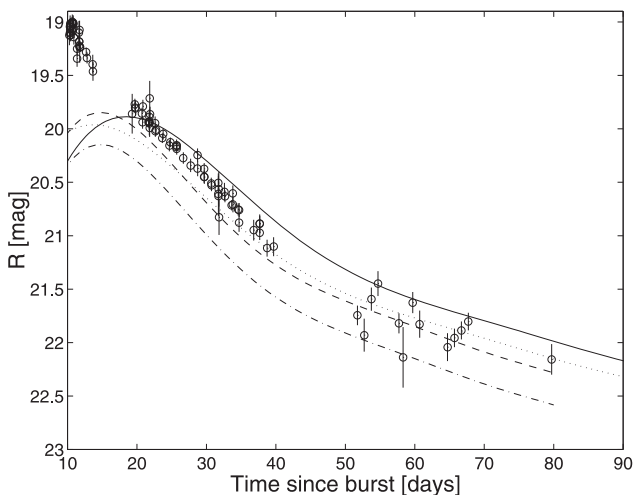


FIG. 2.—Host-subtracted  $R$ -band light curve of the OT (*open circles*) compared with four model light curves of SN 2003dh. The plotted lines are the light curve of SN 1998bw, redshifted and  $K$ -corrected (*solid line*); the same model, after application of the best-fitting magnitude shift and temporal shift relative to the GRB (see text; *dotted line*); the same model, after application of the best-fitting magnitude shift and stretch correction (see text; *dashed line*); and the time-stretched and magnitude-shifted model lowered by 0.3 mag (*dash-dotted line*).

assuming it exploded simultaneously with the GRB. This simple model is consistently brighter than the data points after day  $\sim 20$  and is therefore ruled out—had SN 2003dh been identical to SN 1998bw, the OT would have been brighter than observed after day 20.

Hjorth et al. (2003) decomposed their observed spectra into an SN Ic component (by using redshifted versions of SN 1998bw spectra) and a power-law component, typical for the optical emission from cosmological GRBs. Using this method, these authors derived a  $V$ -band light curve of the SN component during the first month after the GRB. They found that their data could not be fitted by a redshifted and  $K$ -corrected  $V$ -band light curve of SN 1998bw (see their Fig. 3) but required that the SN component be slightly brighter (by  $\sim 0.2$  mag) at the peak and also decline much faster than SN 1998bw, becoming at least 0.7 mag fainter 28 days after the GRB. Similar results were obtained by Mazzali et al. (2003), who combined spectral analysis with explosion models.

With this in mind, we consider alternative models for the SN component. Following Hjorth et al. (2003) and motivated by theoretical models of delayed core collapse (e.g., Vietri & Stella 1998; Berezhiani et al. 2003), we consider a nonsimultaneous SN model. The model light curve (Fig. 2, *dotted line*) was obtained by fitting the  $V$ -band light curve of SN 1998bw to that of SN 2003dh (Hjorth et al. 2003) with two free parameters: a time lag between the GRB and the SN explosion ( $\Delta T$ ) and a magnitude correction ( $\Delta m$ ). The best-fit values are  $\Delta T = -4.7^{+1.7}_{-2.2}$  days and  $\Delta m = 0.08 \pm 0.10$  mag, with  $\chi^2/\text{dof} = 2.5/4$ . This model initially agrees with the data but becomes too bright after day 50 and is therefore discarded. Larger temporal offsets (required to make the SN fainter at late times) are inconsistent with the spectral analysis of Stanek et al. (2003), Matheson et al. (2003), and Hjorth et al. (2003). In the next model (Fig. 2, *dashed line*), we introduced a magnitude correction parameter ( $\Delta m$ ) and a “stretch” parameter  $s$  (similar to the formalism used by Perlmutter et al. 1999), which adjusts the width of the light curve so that the model luminosity of SN 2003dh at time  $t$  after the burst is given by the luminosity of the redshifted SN 1998bw at  $t/s$ . We find  $s = 0.80 \pm 0.05$  and  $\Delta m = -0.01 \pm 0.10$  (with  $\chi^2/\text{dof} = 0.9/4$ ) by fitting the  $V$ -band light curve of SN 1998bw to the measurements of Hjorth et al. (2003). This model provides a somewhat better fit to the data compared with the delayed-GRB model (*dotted line*) but still overestimates the data after day 50.

In search for an SN model that satisfies all available constraints, we consider two additional inputs. Bloom et al. (2004) used a self-consistent multicolor data set obtained with a single instrument (ANDICAM, mounted on the Cerro Tololo Inter-American Observatory [CTIO] 1.3 m telescope). They found that their data could be adequately modeled by using the redshifted and  $K$ -corrected light curves of an SN 1998bw-like event that is slightly brighter than SN 1998bw. Such light curves are ruled out by our measurements, obtained from day 20 onward. The probable reason for SN 1998bw being consistent with the observations of Bloom et al. (2004) is that their data are well sampled until day 12, and their latest data points were obtained at day 23, just when our data start indicating that SN 1998bw-like light curves are too bright.

Matheson et al. (2003) did not pursue the full calculation of  $K$ -corrections required to produce the light curves of SN 1998bw as they would appear for an event exploding at  $z = 0.1685$ . Instead, they used the  $V$ -band light curve of

SN 1998bw as a proxy for the  $R$ -band light curve of SN 2003dh. Comparing their adopted “ $R$ -band” light curve with the results of our own calculation, we find that their light curve has a similar shape but is fainter by  $\sim 0.4$  mag, taking into account their estimated extinction  $A_R < 0.2$  mag. In their SN light-curve model, Matheson et al. (2003) further scaled down SN 2003dh by  $\sim 0.2$  mag, relative to their adopted SN 1998bw light curves. Thus, the good fit they reported for SN 1998bw-like light curves is actually for an event fainter by  $\sim 0.6$  mag.

Because our late-time data rule out nonstretched SN 1998bw-like light curves, even if they are as faint as advocated by Matheson et al. (2003), we are led to construct a model that is identical to the stretched model (Fig. 2, *dashed line*) but is attenuated by 0.3 mag (Fig. 2, *dash-dotted line*), a compromise between the results of Bloom et al. (2004) and Hjorth et al. (2003), suggesting peak magnitudes at least as bright as those of SN 1998bw, and those of Matheson et al. (2003), who found that SN 2003dh was fainter than SN 1998bw by  $\sim 0.6$  mag. This last model seems to best fit both our data and other available studies and is also in good agreement with the theoretical modeling reported by Mazzali et al. (2003). Both the attenuation factor and the stretch parameter of this last model are well situated in the parameter space of fitted 1998bw-like SNe, which was obtained by Zeh, Klose, & Hartmann (2003) for a sample of seven GRB optical counterparts. Note that we do not correct for the host galaxy extinction of SN 2003dh. If we assume negligible extinction of SN 1998bw and the maximal extinction values allowed by the analysis of Matheson et al. (2003) and Bloom et al. (2004),  $A_V \lesssim 0.4$ , our adopted peak magnitude may be consistent with that of an SN that is intrinsically identical to SN 1998bw. The  $\Delta m = 0.3$  mag we adopted for the attenuation of SN 2003dh relative to SN 1998bw is, in fact, a lower limit on the attenuation (or conversely, an upper limit on the allowed peak luminosity). Therefore, below we further check the robustness of our results to the value of attenuation we adopt in our SN model.

### 3.2. The Afterglow Component

The clear-cut connection between GRB 030329 and SN 2003dh makes it important to characterize the afterglow in detail, in order to check whether this is a typical burst or an exceptional one. Figure 3 shows the  $R$ -band light curve of the afterglow, derived by subtracting the host galaxy flux and the preferred SN model (Fig. 2, *dash-dotted line*; see § 3.1 for details). The afterglow light curve is clearly not a smooth decline—strong variations are apparent, starting very early after the burst and continuing throughout our observations (§ 3.3). Inspection by eye shows that the early light curve may be described by a power-law decline, with a steepening of the slope around  $t \sim 5$  days.

We therefore begin our examination by investigating the simplest plausible model—a singly broken power law. We fitted sets of double power laws to the afterglow light curve. In each fit, we assumed a different break time  $t_{\text{brk}}^{\text{asu}}$  (i.e., one power law was fitted to all the points with  $t < t_{\text{brk}}^{\text{asu}}$  and another one to points with  $t > t_{\text{brk}}^{\text{asu}}$ ). The intersection time ( $t_x$ ) of the two power laws and the sum of the  $\chi^2$  values of the two fits were calculated for each  $t_{\text{brk}}^{\text{asu}}$ . During the first 3 days, the light curve was sampled more intensively than at later times. To reduce the overwhelming statistical weight of this segment, we diluted it by binning the points. The dashed lines in Figure 3 are a few examples of such fits, with  $t_{\text{brk}}^{\text{asu}} = 3, 5,$  and 8 days.

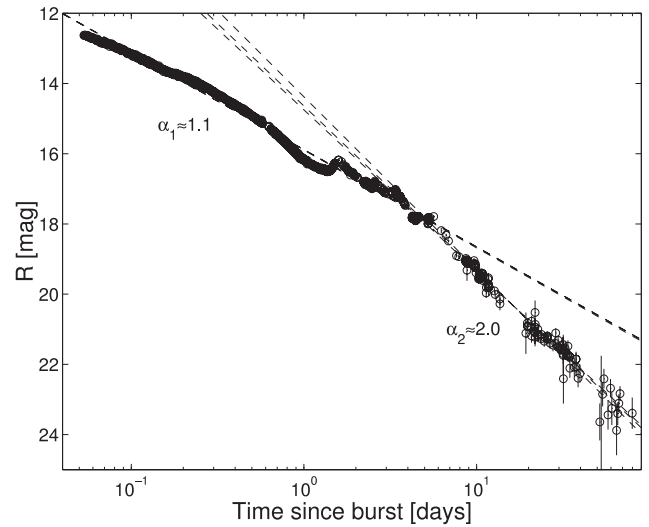


FIG. 3.— $R$ -band light curve of the afterglow. The light curve was derived by subtracting the contribution of SN 2003dh and of the host galaxy from the observed light curve. Overlaid are a few power-law fits to early and late times (see text for details). A break at  $t \sim 5$  days is apparent. The slope of the prebreak power law is  $\alpha_1 \approx 1.1$ , and that of the postbreak is  $\alpha_2 \approx 2.0$ .

As can be seen, the values of the early- and late-time slopes are weakly dependent on the assumed break time. We therefore consider these values ( $\alpha_1 \approx 1.1$  and  $\alpha_2 \approx 2.0$ , where  $\alpha$  is the power-law decay index defined by the dependence of flux,  $f$ , on time  $f \propto t^{-\alpha}$ ) to be robustly constrained by the data.

For assumed break times between 1.5 and 11 days, the calculated intersection between the two power-law fits falls consistently between 3 and 5 days. Minimum  $\chi^2$  values were obtained for assumed breaks between 3 and 6 days. When carried out with light curves in the  $B$ ,  $V$ , and  $I$  bands, the same procedure yielded a similar range for the intersection points:  $3 \text{ days} \leq t_x \leq 8 \text{ days}$ .

To test the sensitivity of our results to the SN model that was subtracted from the light curve, we repeated the test using several different SN models. All the models were redshift- and  $K$ -corrected light curves of SN 1998bw, stretched by  $s = 0.80$ . We varied the values of the attenuation  $\Delta m$  in the range  $0.3 \text{ mag} \leq \Delta m \leq 0.6 \text{ mag}$ , since brighter values ( $\Delta m < 0.3$ ) are ruled out by our light curves (see § 3.1) and fainter values ( $\Delta m > 0.6$ ) are inconsistent with the strength of the observed SN features in the OT spectra (Matheson et al. 2003; Hjorth et al. 2003). The early-time slope did not change significantly, while the late-time slope varied between 1.8 and 2.0, leaving the range of intersection times unchanged.

To conclude, for a singly broken power-law model, our data robustly constrain the early- and late-time decay slopes to lie around  $\alpha_1 \approx 1.1$  and  $\alpha_2 \approx 2.0$ , respectively. These values depend very weakly on the light-curve segments used or on the SN model subtracted. If we take the intersection time of these slopes as an estimate for the break time, the resulting values lie around  $t \sim 5$  days. However, because of the strong variations in the light curve, the time of the break is not well constrained and could be placed at any time between  $\sim 3$  and  $\sim 8$  days. If we adopt  $t_{\text{brk}} = 5$  days for the time of the break, a fit to the data before and after the break yields  $\alpha_1 = 1.11 \pm 0.01$  and  $\alpha_2 = 1.96 \pm 0.02$ . The intersection of these two power laws,  $t_x = 4.9$  days, is self-consistent with the

assumed  $t_{\text{brk}}$ . This result agrees with the late-time power-law slope,  $\alpha = 2.05$ , measured by Matheson et al. (2003) from data obtained between  $t \approx 5$  and  $\approx 61$  days. It appears that a double power law, broken somewhere between day  $\sim 3$  and  $\sim 8$  and strongly perturbed by a series of bumps (Figs. 3 and 4), provides a fair description of the complex light curve of this OT. We therefore continue and analyze the properties of the variable component derived from the simple broken power-law model in the next section.

Numerous works, analyzing short or sparsely sampled optical light curves, have interpreted some of the deviations from a smooth decline observed in the OT light curves as manifestations of specific phenomena predicted by popular relativistic jet models. In particular, Berger et al. (2003) propose a model that attempts to consistently account for observations in the radio, millimeter, optical, and X-ray bands. We review the complex structure seen in our superior data in the context of previous analyses in § 4.1 below and confront an updated version of the Berger et al. (2003) model with our optical observations in § 4.2.

### 3.3. The Variable Component

Subtracting our best double power-law decline model (§ 3.2) from the afterglow light curve, we derive the residual  $R$ -band light curve of the afterglow. Three segments of the residual light curve are shown in Figures 4, 6, and 7.

Figure 4 shows the residual light curve during the first 8 days after the burst. Arbitrarily, we consider the variability as a series of bumps, although with no model at hand, this is a mere matter of convenience. The bumps in Figure 4 are marked according to the notation introduced by Granot, Nakar, & Piran (2003), who identified four bumps in the light curve of the OT, compiled from reports in GCN Circulars ( $A$ ,  $B$ ,  $C$ , and  $D$  in Fig. 4). The early bump,  $\aleph$ , was identified by Uemura et al. (2003), and the minor bumps,  $A'$  and  $C'$ , are introduced in this work. The validity of the minor bump  $C'$  is uncertain because the peak of the bump is only  $\sim 1 \sigma$  brighter than the dip prior to the bump and since the points forming its peak all come from the same data set (Matheson et al 2003). The bumps before day  $\sim 8$ , which possibly occurred prior to the change in the afterglow decline rate (Fig. 4; see

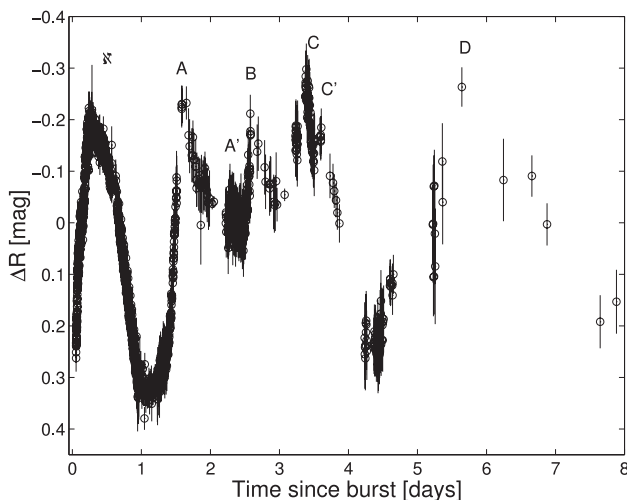


FIG. 4.—Residual light curve obtained by subtracting our best-fit double power law (see text) from the light curve of the afterglow, during the first 8 days after the burst. Five strong bumps, along with two possible minor ones, are apparent in the light curve.

§ 4.3 below), are asymmetric in shape, with an incline that is typically  $\sim 2$  times as steep as the decline (with the possible exception of  $C'$ , which is poorly sampled).

Bumps  $A$ ,  $B$ , and  $C$  share a strikingly similar overall structure and timescale during  $\sim 0.6$  days about their maximum. This similarity is demonstrated in Figures 5a, 5b, and 5c, where each of the three bumps is shown compared with a curve manifesting the common coarse structure of these bumps. To derive this “standard profile” of the bumps, we superposed bumps  $B$  and  $C$  over bump  $A$ . Bumps  $B$  and  $C$  were shifted by  $\Delta T = -1.02$  days,  $\Delta m = -0.008$  mag, and  $\Delta T = -1.718$  days,  $\Delta m = 0.055$  mag, respectively, to obtain a good match by eye. The data were then smoothed by using cubic splines. Finally, we derived a profile curve by using a high-degree polynomial fit.<sup>13</sup>

The three events are consistent with this standard profile, composed of a fast monotonic rise and a slower, complex decline. Figures 5d, 5e, and 5f show a comparison between the standard profile and bumps  $\aleph$ ,  $A'$ , and  $D$ , respectively. The brightening rate of bump  $\aleph$ , as well as its timescale, is similar to the standard profile. However, its structure is significantly different. In particular, in contrast to the concave early decline that  $A$ ,  $B$ , and  $C$  seem to share, the declining branch of bump  $\aleph$  has a convex form. Our fragmented data of bump  $D$  are consistent with the standard profile but on a timescale that is longer by a factor of  $\sim 2$ – $2.5$ . Finally, the rising branch of minor bump  $A'$  seems to be similar to the tip of the standard profile, but its decline is slower, perhaps because of the rising of bump  $B$ .

Another apparent phase of variability, between 8 and 13 days, features three consecutive low-amplitude ( $\Delta R \approx 0.1$  mag) bumps, with a timescale of  $\sim 1$  day (Fig. 6). However, the amplitudes of the later two bumps ( $t \sim 10.7$  and  $11.7$  days) are within the cross-calibration systematic uncertainties, and their maxima data all come from a single source (Mount Laguna Observatory) and should therefore be treated with caution until confirmed by other observations. A broad bump ( $F$ ) spanning  $\sim 20$  days occurred around  $t \approx 30$  days (Fig. 7). The shape of this feature is somewhat sensitive to the SN model used. Nevertheless, the deviation from the power-law decline during this period persists for any of the SN models that we have tested.

Strong variability is also detectable during the late decline, after  $t \sim 50$  days. In particular, a  $\sim 0.3$  mag rebrightening on a timescale of 2 days occurred around  $t \approx 52$  days (the “jitter episode” of Matheson et al. 2003; see Fig. 3). Our light curve features another  $\sim 0.2$  mag rebrightening on a timescale of a few days, around  $t \approx 64$  days. Because the observations tracing this variation were all obtained at the same observatory (MDM 2.4 m), it is unlikely that this is due to some reduction artifact. To conclude, it appears that successful models of this well-observed GRB should ultimately account for strong variations of the optical emission, on timescales of hours to weeks, recurring over tens of days after the burst.

### 3.4. Color Evolution

Figure 8 shows the  $B$ – $R$  color evolution of the light curve of GRB 030329. The host and the SN light curve were not subtracted, in order to reduce propagated errors and keep the

<sup>13</sup> A tabulated version of the “standard profile” is available at <http://wise-obs.tau.ac.il/GRB030329>.

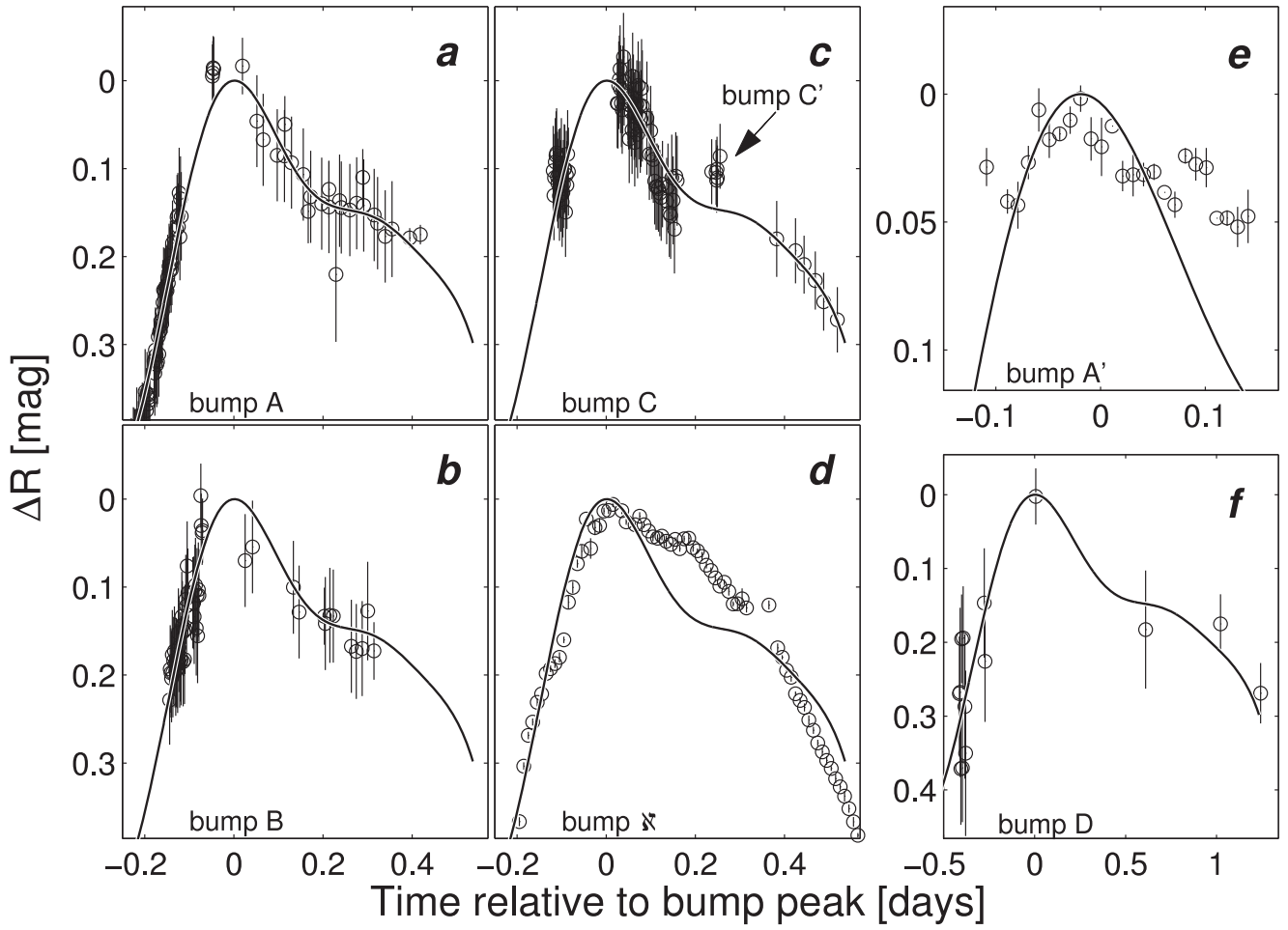


FIG. 5.—Close-up view of the main bumps detected in the early residual light curve, which was obtained by subtracting our best-fit double power law (see text) from the light curve of the afterglow. (*a–f*) Bumps *A*, *B*, *C*,  $\xi$ , *A'*, and *D*, respectively. The light curves in (*d*) and (*e*) were binned to allow convenient browsing. The solid curves are a smoothed fit to the superposed light curves of bumps *A*, *B*, and *C*, representing the common structure of these three bumps (see text for details). The timescale of the curve in (*f*) was stretched by a factor of 2.3.

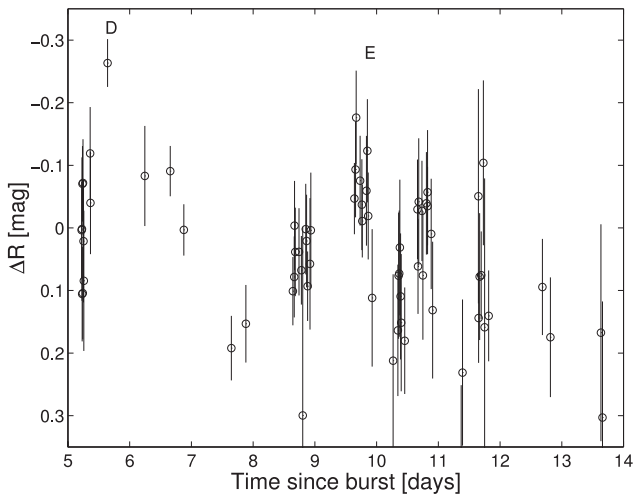


FIG. 6.—Variations light curve of the afterglow between day 5 and day 14

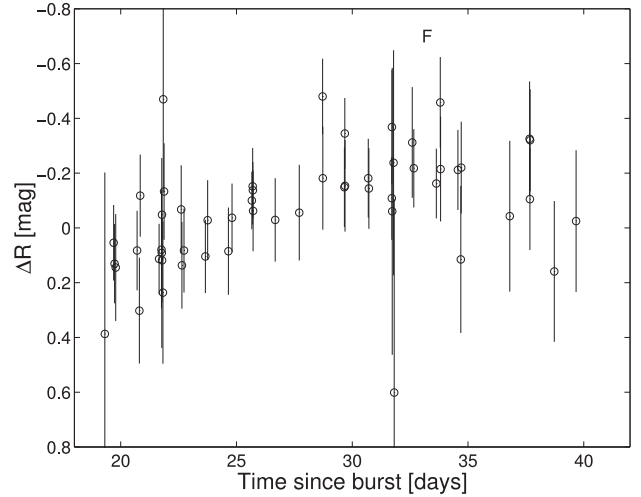


FIG. 7.—Variations light curve of the afterglow between day 18 and day 42

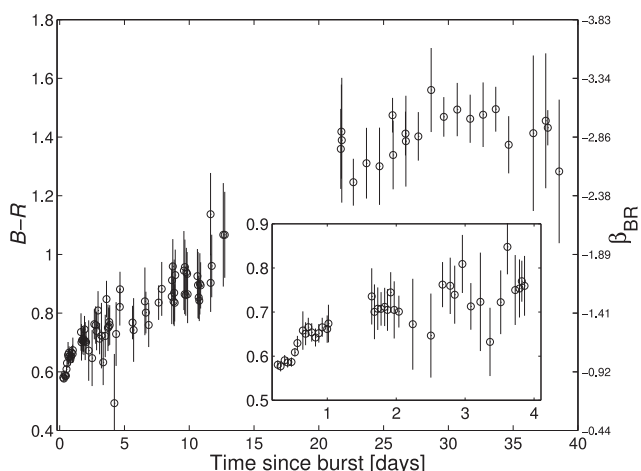


Fig. 8.—Binned  $B-R$  color of the OT during the first 40 days after the burst. The vertical axis on the right shows the corresponding spectral power law,  $\beta_{BR}$ . The inset is a blowup of the first 4 days.

results model independent. To derive the  $B-R$  light curve we interpolated the better sampled  $R$ -band light curve onto the times of the  $B$ -band light curve. The interpolation uncertainty was calculated by using the method of Ofek & Maoz (2003). Finally, we binned the  $B-R$  color light curves in 0.05 day bins.

The color evolution of this event was studied in detail by Matheson et al. (2003) and Bloom et al. (2004). Both groups used subsets of the data presented here. Our analysis yields consistent results with those previous works. In particular, we measure almost constant colors between days 2 and 5, after which the emerging SN component (with colors similar to SN 1998bw) drove the color evolution of the optical emission. Furthermore, the earlier coverage of our light curves enables us to measure the color evolution of the OT during the first day.

The  $B-R$  light curve shows a small ( $\sim 0.1$  mag) but significant color variation during the first day after the burst (Fig. 8, *inset*). The color of the OT evolved from  $B-R = 0.58 \pm 0.01$  mag at  $t = 0.28$  days (corresponding to  $\beta_{BR} = -0.88 \pm 0.02$ ) to  $B-R = 0.66 \pm 0.02$  mag at  $t = 0.83$  days (corresponding to  $\beta_{BR} = -1.07 \pm 0.05$ ), where  $\beta_{BR}$  is the spectral energy slope defined by  $f_\nu \propto \nu^\beta$  (where  $f_\nu$  is the specific flux). This early evolution is unlikely to be related to the SN component. To date, color evolution has been observed in the light curves of GRB 021004, starting  $\sim 1.5$  days after the burst (Bersier et al. 2003; Mirabal et al. 2003), and possibly also in GRB 000301C (Rhoads & Fruchter 2001). An interpretation of the color change of GRB 030329 in the context of the relativistic synchrotron model, as a manifestation of the cooling-break frequency going through the optical bands (e.g., Galama et al. 2003), is discussed below (see § 4.1).

## 4. DISCUSSION

### 4.1. Early Breaks

The relative proximity of GRB 030329 has prompted special attention by the astronomical community, and several works presenting analysis of various data sets have been published so far. Our superior compilation of optical data, as well as the privilege afforded by the availability of these

earlier works, allows us to inspect some previous suggestions in light of the newly available data.

Early analysis of preliminary optical data revealed that the slope of the optical decline became steeper around day 0.5–0.6 (e.g. Garnavich, Stanek, & Berlind 2003a; Burenin et al. 2003; Price et al. 2003b). The change in the power-law decline index from  $\sim 1$  to  $\sim 2$ , seen both in early optical data and in sparse X-ray observations reported by Tiengo et al. (2003), combined with the achromatic nature of the break (Burenin et al. 2003), seemed to support an interpretation of this steepening as a “jet break,” the manifestation of a conical geometry in the relativistic emitting material (e.g., Rhoads 1997).

Figures 3 and 9 show that this simple interpretation does not fit the well-sampled light curves now available. A model postulating a steep ( $\alpha \sim 2$ ) optical decline starting at day  $\sim 0.5$  would severely underpredict the optical observations from day 1.5 onward. Sustaining a model involving a jet break at day 0.5 requires an additional source of optical emission emerging at day  $\sim 1$ . Such a model was indeed suggested by Granot et al. (2003) and Berger et al. (2003) and is discussed in the next section.

As can be seen in Figures 4 and 9, as well as in Uemura et al. (2003) and Sato et al. (2003), the early optical data (i.e., before the suggested break at day  $\sim 0.5$ ) are not consistent with a single power-law decline, as predicted before a jet break. In particular, the data presented by Uemura et al. (2003), Torii et al. (2003), and Sato et al. (2003) require at least one additional break to occur around day  $\sim 0.25$ . Our compilation clearly elucidates this (Fig. 9). Several authors (Torii et al. 2003; Sato et al. 2003) suggested that this additional break (with a change in the temporal slope of  $\Delta\alpha \sim 0.3$ ) may represent the so-called cooling break, predicted in the context of relativistic fireball models (Sari, Piran, & Narayan 1998) to occur as the cooling-break frequency,  $\nu_c$ , passes through the optical band (with  $\Delta\alpha = 0.25$ ). As seen in

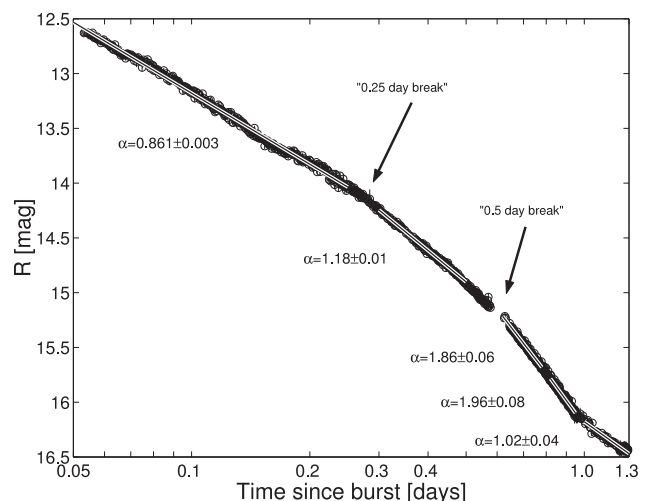


Fig. 9.—Detailed view of the early light curve of the OT associated with GRB 030329. The light curve distinctly breaks around 0.25 and 0.5 days. The data obtained prior to 0.25 days is not well described by a smooth power law and shows significant wiggles. Note that our data rule out further steepening of the light curve at day 0.8, with the slope measured during 0.82–0.95 days consistent with the slope measured from earlier data (0.6–0.78 days) and certainly below the values  $\alpha \sim 2.2$  reported elsewhere (see text). Around day 1 the decline in the optical flux begins to slow, as the rising branch of bump A emerges.

Figure 9, the combination of an early cooling break at day 0.25 and a jet break at day 0.5 allows a fair representation of the *early* optical data. Thus, successful models of this event should account for at least two early breaks. However, it should be stressed that the well-sampled light curves available before 0.25 days are not consistent with a smooth power-law decline and show significant wiggles and bumps (we discuss this point further below).

Previous studies suggesting an early cooling break relied on the analysis of single-band data and could therefore detect only the predicted shift in the temporal decay slope  $\alpha$ , as discussed above. Our compilation also allows us to inspect the color evolution of the OT around the time of the suggested cooling break. As reported in § 3.4, we detect a shift in the optical spectral index of  $\Delta\beta = 0.19 \pm 0.05$  between 0.28 (our earliest available color data) and 0.83 days after the burst.

Relativistic synchrotron models predict that a cooling break sweeping the optical band would manifest itself by a change in the color index of  $\Delta\beta = 0.5$ . If the observed color change is indeed due to the cooling break, then considering that  $\sim 40\%$  of the expected color change occurred between 0.28 and 0.83 days and noting that both theory (Sari et al. 1998) and observations (Galama et al. 2003) show that the cooling break evolves in time with a power law, we estimate that the cooling break crossed the  $V$  band at day  $\sim 0.25$ . We note that the observed steepening of the slope passed through the optical band from high frequencies to low ones and hence demotes models predicting an opposite trend.

Another way to probe the cooling-break frequency value during later times is through the optical-to-X-ray spectral index, which is predicted to be constant after the cooling break moves below the optical bands. We measured this in four epochs of *RXTE* and *XMM-Newton* observations given by Tiengo et al. (2003;  $t = 0.222, 1.24, 37.24,$  and  $60.85$  days; the first epoch is the weighted mean of four measurements), by interpolating the  $R$ -band afterglow light curves onto the four epochs of the X-ray observations.

The value of the slope at the first epoch,  $-0.93 \pm 0.02$  (at  $t = 0.222$ ), before or during the proposed cooling transition, differs markedly from the values obtained at later epochs, after the break,  $-1.04 \pm 0.05$  and  $-1.06 \pm 0.13$  at 37.24 and 60.85 days after the burst, respectively. The value measured 1.24 days after the burst,  $-0.95 \pm 0.04$ , is consistent with both early and later values. A coherent picture therefore emerges from the optical observations and X-ray data in which the color evolution we detected is possibly the result of the cooling-break passage through the optical band around 0.25 days after the burst. Naturally, other explanations for the observed early color evolution are possible.

Finally, we consider the report by Smith et al. (2003) of a further steepening of the optical light curve (reaching  $\alpha \sim 2.2$ ) around 0.8 days that is distinct from and occurring after the proposed 0.5 days break. This could have confirmed the prediction by Granot et al. (2003) that the final slope after a jet break around 0.5 days should be steeper than the value reported ( $\alpha = 1.9$ ), as expected from the temporal slope change due to a jet break,  $\Delta\alpha \sim 1$ , relative to the post-cooling-break slope  $\alpha \sim 1.2$ . However, our superior data, including two mutually consistent data sets from the MDM and Mount Laguna Observatory, obtained through standard filters, are not consistent with the unfiltered data reported by Smith et al. (2003). Figure 9 shows no segment of the early light curve (including the period between 0.8 and 1 day) with

a power-law slope steeper than  $\alpha = 2$ . Thus, the theoretically predicted slope of  $\alpha = 2.2$  either was not reached or was washed out by the emerging bump  $A$ .

To conclude, our results support the interpretation of the break around 0.25 days as a cooling break, within the context of relativistic synchrotron models. The interpretation of later steepening of the light curve (around 0.5 days) as associated with a geometric (“jet”) break can be sustained only if an additional emission source, dominating the optical flux from day 1.5 onward, is invoked.

It should also be noted that Dado, Dar, & De Rújula (2003) also put forward a theoretical prediction for the optical light curves of this event, based on their “cannonball” model. Lacking access to the predicted curves, we are unable to conduct a detailed comparison with our data. However, such a comparison is certainly warranted and could be easily conducted by using our publicly available data.

#### 4.2. The Two-Jet Model Revisited

Berger et al. (2003) analyzed radio observations of GRB 030329 and found that the radio data, as well as millimeter-band observations reported by Sheth et al. (2003), could be well described by a relativistic jet model. However, the jet parameters indicated a “wide” jet, exhibiting the characteristic jet break about 10 days after the burst. In view of previous analysis of early optical and X-ray data, which seemed to require a “narrow” jet, breaking around day 0.5, Berger et al. (2003) proposed a composite two-jet model, combining a narrow ultrarelativistic component responsible for the gamma rays and early ( $t \lesssim 1.5$  days) optical and X-ray afterglow with a wide, mildly relativistic component responsible for the radio and optical afterglow beyond 1.5 days. This model provides a good fit to the radio and millimeter data as well as to the preliminary optical data used by these authors. The model also describes well the early X-ray observations but underestimates late ones. The wide jet component provides the additional source of emission required to account for the optical observations after day 1.5, as discussed above.

The energy derived from the Frail relation (Frail et al 2001; Bloom et al. 2004), assuming only a narrow-jet component and the updated parameters used by Bloom et al. (2004), falls  $7\sigma$  below the geometrically corrected mean gamma-ray energy of Bloom et al. (2004). The contribution of the wide-jet component introduced by Berger et al. (2003) brings the total energy to within  $1\sigma$  of the mean value of Bloom et al. (2004).

With our improved optical light curves at hand, we revisit the Berger two-jet model. Figure 10 shows a comparison between an updated two-jet model with radio data from Berger et al. (2003) and X-ray data from Tiengo et al. (2003), as well as our  $R$ -band light curve. The model is essentially the same as the one described in Berger et al. (2003), except for the following modifications. First, a cooling-break component at 0.25 day (see § 4.1) was incorporated into the model. In addition, the temporal emergence of the second jet at  $t \sim 1.5$  days was set to  $t^4$  (instead of the  $t^2$  law used in Berger et al. 2003) to account for the abrupt rise that our nearly continuous data show (in fact, an even steeper emergence is probably required). Finally, the 1998bw-based SN model used by Berger et al. (2003), which we showed to be too bright, was replaced by our best SN model as described in § 3.1.

The modified two-jet model fairly describes the trends in our well-sampled optical light curves. However, some

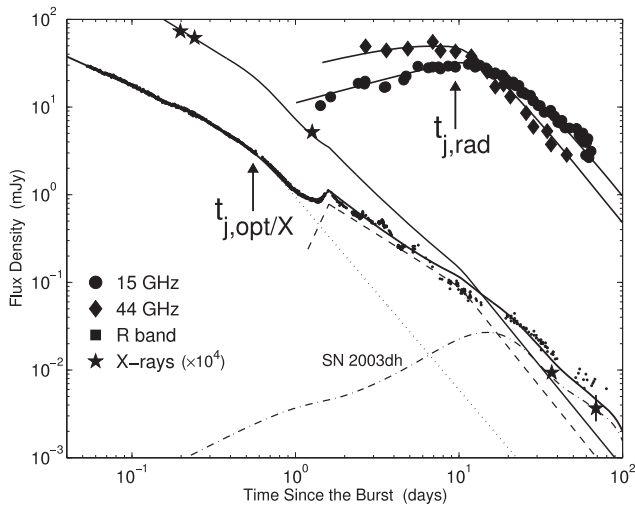


FIG. 10.—Comparison of the updated two-jet model with multiband data. The model and notation are similar to those presented by Berger et al. (2003), except for several minor modifications (see text). Symbols denote data points, as labeled, and the solid curves are the model predictions in each respective band. The model *R*-band light curve describes the trends in the observed light curve well, but some discrepancies remain—the model becomes too bright around 10 days after the burst and later on becomes too faint.

discrepancies still remain. Figure 11 shows the residuals obtained by subtracting the updated two-jet model from the observed *R*-band light curve. At early times ( $\lesssim 1.5$  days), the model fits the trends in the light curve. Nevertheless, significant undulations (with peak to peak  $\gtrsim 0.1$  mag) are detected about the smooth model (Fig. 12). Thus, this or any other model based on broken power-law segments should ultimately be supplemented with a mechanism explaining the bumpy nature of the optical emission, starting at the very earliest

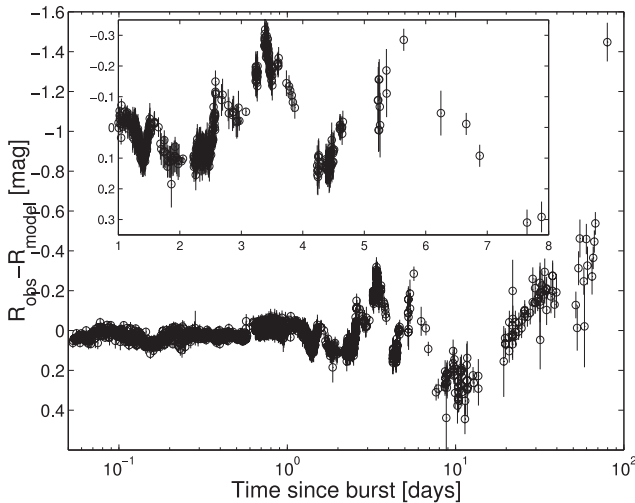


FIG. 11.—Residual light curve obtained by subtracting the modified two-jet model from the observed *R*-band light curve. Note that at  $t \leq 1$  day the model describes the light curve trends very well, but significant wiggles around the smooth trend remain. A phase of strong variations can be seen between 1 and 8 days, followed by broader undulation around the predicted peak of SN 2003dh, that may be associated with inadequacies in the SN model. During later times ( $\gtrsim 20$  days), the data seem to require yet another source of optical emission, which is also strongly variable. The inset is a magnified view of the strong variations between day 1 and day 8.

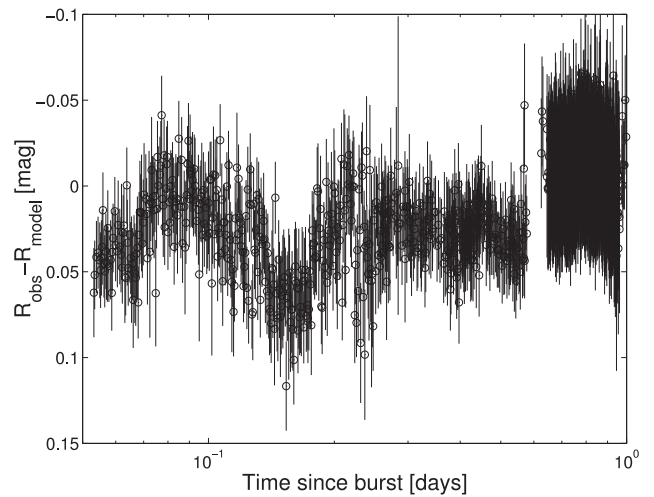


FIG. 12.—Same as Fig. 11, but zooming in on the period prior to the emergence of bump *A*. The residual undulations after subtraction of the Berger et al. (2003) two-jet model light curve are clearly evident.

times (e.g., even prior to the cooling break). Following, a period of strong variations ensues, lasting till day 8. Comparing the inset in Figure 11 with Figure 4, we see that the two-jet model eliminates bump *N* (which under this interpretation is the combined effect of the cooling and jet breaks), while bump *A*, associated with the emergence of the second jet, is diminished. However, later structure, including bumps *B*, *C*, and *D*, remains. Moreover, both the structure of these bumps and their peak-to-peak amplitude are essentially unaltered. Thus, the modified two-jet model does not eliminate the need for an additional strongly variable component of optical emission.

After day 8, a smooth undulation, lasting until day  $\sim 20$ , is seen in Figure 11. Since this is the period in which the optical flux is dominated by the emission from SN 2003dh, the discrepancy seen may indicate that our model light curve of SN 2003dh is at fault. This undulation can be almost completely removed by making our model for SN 2003dh fainter by 0.3 mag—at the lower limit of the range we consider plausible (see § 3.1).

Finally, the data clearly require an additional source of optical flux in order to explain the late-time ( $\gtrsim 20$  days) light curve. This extra component (in addition to the narrow and wide jets and SN 2003dh) should rise from day 20 through day 79, where our data end, and is also required to be strongly variable in order to explain the late-time light-curve “jitters.” This extra flux cannot be attributed to the SN without making its light curve very different from that of SN 1998bw and highly variable. Further tests for the relative contribution of SN 2003dh to the late-time optical flux can be obtained from late-time spectroscopy of this event. Interestingly, as can be seen in the lower right corner of Figure 10, the modified two-jet model also underpredicts the late-time X-ray points (at  $t = 37.24$  and  $60.85$  days), perhaps indicating a need for an extra source of late-time flux in this band also.

To conclude, as already shown by Berger et al. (2003), the two-jet model provides a fair, self-consistent description of observational data from the radio to the X-ray. However, in view of the large volume and complex nature of the multi-band data obtained for this event, further investigation of

this model, perhaps combined with a prescription for the additional variations component required, is warranted.

#### 4.3. Can a Single Broken Power Law Provide a Good Fit to the Data?

We demonstrated above that if we assume a power-law decline—the simplest OT model commonly used—the data require different slopes for the early- and late-time declines (§ 3.2). The values of the decline indices,  $\alpha_1 \approx 1.1$  and  $\alpha_2 \approx 2$ , are robustly constrained by the data. The transition between these decline slopes requires a break in the optical light curve  $\sim 3$  to  $\sim 8$  days after the burst. Unfortunately, the strong undulations superposed on the smooth decline trend throughout this period prevent us from determining the accurate timing of the power-law break.

It is intriguing to test whether this simple model, which naturally emerges from the analysis of the optical data, can consistently provide a reasonable fit to the entire multi-band data set gathered for this burst. In this context, we note the following major points. In the optical regime, this simple model for the “smooth” evolution of the OT requires (an) additional emission component(s) to account for the strong flux variability detected from hours to weeks after the burst. The ubiquity of these undulations suggests that such a component cannot be avoided by more complex models that have thus far been proposed. Particularly, as shown (§ 4.2), the two-jet model advocated by Berger et al. (2003) accounts for some of the more prominent features in the optical light curves of this event ( $N$  and  $A$  in Fig. 4) but does not account for other, equally prominent ones. Thus, without concrete and self-consistent models for the mechanism of the light-curve variability, the amplitude of the undulations about the simple broken power-law model for this burst does not seem to argue against the validity of the single-break model.

The X-ray coverage of this burst is regrettably sparse. Comparing the available data reported by Tiengo et al. (2003) with our optical light curves and assuming that the X-ray and optical flux are correlated, as found by Fox et al. (2003) for GRB 021004, we expect the optical-to-X-ray slope index to remain approximately constant. As we have shown in § 4.1, this is indeed the case, especially if the early X-ray point, obtained before the proposed cooling transition, is discarded. We note, however, that when overplotting the X-ray data on the  $R$ -band light curve and scaling the X-ray points to match the early light curve, the two latest *XMM* points fall below their expected position by a factor of 6–10. The physical significance of this discrepancy is not clear. We note, however, that a discrepancy of similar magnitude (but of opposite direction) is also found when one compares the modified two-jet model (§ 4.2) with the X-ray data (Fig. 10, *bottom right*). If any of these models is correct, this may suggest a weak evolution in the optical-to-X-ray spectral slope.

Finally, it appears that the greatest challenge for the simple one-break model is accounting for the results of the radio and millimeter observations. As elaborated by Berger et al. (2003), these data require the existence of a mildly relativistic jet, which is expected to demonstrate a break in the optical regime around day 10 after the burst. Thus, the single break between  $\sim 3$  and  $\sim 8$  days after the burst implied by the simple model seems to be somewhat at odds with the constraints posed by the radio and millimeter data. However, no confidence intervals have been determined for the timing of the

break, both in the optical and in radio. In the optical band, the measurement is hindered by strong, multiple bumps and wiggles superposed on the smooth light curves. The apparent conflict in the determination of the break time may perhaps be negotiated by future analysis, which would also model the variations in the optical band (e.g., by fitting a physically motivated model explaining the observed optical light curves). We thus conclude that the data at hand cannot rule out the empirically motivated singly broken power-law model for the emission associated with GRB 030329. Assuming this model with  $t_{\text{brk}} \approx 8$  days,  $E_{\text{iso}}(\gamma)$  as found in § 4.2, and an interstellar matter density  $n = 1.8 \text{ cm}^{-3}$  (Berger et al. 2003), the estimated total energy of the event, derived by using the Frail relation (Frail et al. 2001; Bloom et al. 2004), is  $4.4 \times 10^{50}$  ergs. This value is within  $1.5 \sigma$  of the updated geometrically corrected mean gamma-ray energy value of Bloom et al. (2004).

#### 4.4. Light-Curve Variations

As shown above, the optical light curves of the OT associated with GRB 030329 exhibit strong undulations superposed on the overall smooth trends, detectable shortly (hours) after the burst and still apparent many tens of days later. The variations seen during the period that is best sampled by our light curves have a typical timescale of  $\sim 1$  day and show a similar asymmetric structure, with a rising branch about twice as steep as the declining one. Both the characteristic amplitude ( $\sim 50\%$ ) and the structure of these variations are only weakly influenced by our assumptions about the underlying smooth behavior. In particular, similar results are obtained when we assume either the simple, empirically motivated, singly broken power-law model or the more complex two-jet model of Berger et al. (2003; Figs. 4 and 11, *inset*).

Similar undulations have been previously observed in the light curves of OTs associated with GRBs. A short-time variation was detected in the light curves of GRB 000301C (e.g., Masetti et al. 2000; Rhoads & Fruchter 2001; Berger et al. 2000; Sagar et al. 2000). The short timescale and achromatic nature of the variation led Garnavich, Loeb, & Stanek (2000) to suggest that this bump was caused by microlensing of the OT by a star in a foreground galaxy, while a more mundane origin for the bump—nonuniform ambient density—was proposed by Berger et al. (2000). The timescale and structure (fast rise, slow decline) of the bump detected in GRB 000301C are similar to those seen in our light curves of GRB 030329. This, combined with the different structure seen in optical and IR light curves of the OT of GRB 000301C (Sagar et al. 2000), which also leads to a poor fit of the multiband microlensing model to the observed  $R$ -band light curve (Garnavich et al. 2000), suggests that the bump seen in the light curve of GRB 000301C is more likely to be intrinsic to the source than the result of the rare cosmic alignment required for microlensing. More recently, numerous bumps were detected in the light curve of the OT associated with GRB 021004 (e.g., Bersier et al. 2003; Mirabal et al. 2003; Fox et al. 2003). Here, too, the temporal structure and timescale of the bumps is similar to those seen in our light curves of GRB 030329.

A seemingly exceptional case to note is that of GRB 970508, the second burst for which an OT was identified. The OT of this burst (e.g., Galama et al. 1998b) showed a major rebrightening around 1 day after the burst. Following a short rise lasting less than 1 day, the optical emission

underwent a smooth power-law decline over  $\sim 100$  days. The relatively sparse sampling of the light curve of this burst after day 10 does not allow us to determine the exact nature of the light-curve decline during late phases (e.g., search for late jitter periods), but the overall smooth structure and very large amplitude of this rebrightening appear to be quite different from those of the OT associated with GRB 030329 (or from any other OT so far detected).

The common explanations for the short-timescale variations invoke complex density structures around the burst (e.g., Wang & Loeb 2000; Berger et al. 2000; Lazzati et al. 2002), inhomogeneous energy disposition within relativistic conical blast waves (the ‘‘patchy shell’’ model; Kumar & Piran 2000b), and continued injection of energy by the central engine (refreshed shocks; e.g., Rees & Mészáros 1998; Kumar & Piran 2000a). Nakar, Piran, & Granot (2003) performed a detailed theoretical investigation of GRB 021004 and showed that variants of all these models can fit the data, although they preferred a version of the patchy shell model.

Granot et al. (2003) next studied the variability of GRB 030329 by using a preliminary compilation of early optical data. Interpreting our detailed light curves in view of their analysis, we note the following points. The significant variations observed in the light curve before the proposed cooling break at day 0.25 probably argue against variable density models, in agreement with the conclusions of these authors. Interpreting the 0.5 day steepening in the light curve as a jet break, Granot et al. (2003) ruled out the patchy shell model, since it cannot produce strong variations after the entire jet is visible (i.e., after the jet break). Since strong variations are also observed well after day 10 (e.g., the ‘‘jitter episode’’), the patchy shell model cannot explain the late variations observed in the light curve of GRB 030329. However, if the jet break occurred as late as day 8 (e.g., as in the single power-law model), the patchy shell model may explain the strong early variations.

The refreshed shocks scenario (Kumar & Piran 2000a) predicts that if the shocks occurred before the jet spreading, the timescale of the variations would be  $\Delta t \sim t$ . Granot et al. (2003) showed, however, that if the refreshed shocks occurred after the jet spreading, the timescale of the variations would be  $\Delta t \sim t^{1/4}$ . Considering the roughly constant timescale of the variations and assuming a jet break at day 0.5, Granot et al. (2003) favored the refreshed shocks model for the variations in the light curves of this burst. However, if a jet break occurred after day  $\sim 5$ , the almost constant timescale of the variations would be in contrast with the refreshed shocks model advocated by Granot et al. (2003). Conversely, if refreshed shocks are shown to be the likely mechanism causing the observed variations, a model with a single jet break around day 5 becomes unphysical.

The similar structure of the undulations seen in the light curves of GRB 021004 (Nakar et al. 2003), GRB 000301C (Panaitescu 2001), and GRB 030329 may hint at a ‘‘standard’’ variability mechanism in OTs. Naturally, many more cases should be studied in order to confirm this suggestion.

## 5. SUMMARY

We observed the optical afterglow of the nearby GRB 030329 from five observatories across the globe. We carefully cross-calibrated the observations and augmented them with published data. The final compilation of *BVRI* light curves is unprecedented in its temporal sampling and reveals complex structure.

Decomposing the light curve into host galaxy, SN, and afterglow components, we showed that SN 2003dh, associated with GRB 030329, could not have had a light curve identical to that of SN 1998bw. Instead, the evolution of SN 2003dh is better described by making the light curve of SN 1998bw fainter by 0.3 mag and with a timescale that is 0.8 times shorter. We subtracted this SN model from the light curve of GRB 030329 and found that the residual light curve is well described by a double power law, with a break point in the range of  $\sim 3$  to  $\sim 8$  days. The power-law slope of the light curve changed from  $\alpha_1 \approx 1.1$  to  $\alpha_2 \approx 2.0$ . These results are very weakly dependent on the SN model used.

The SN, host galaxy, and power-law-subtracted light curves of GRB 030329 show strong variations with timescales ranging from  $\sim 0.5$  hr to  $\sim 10$  days. The early variations ( $\lesssim 8$  days), which are well covered by our observations, are typically asymmetric, with their ascending branch about twice as fast as the descending branch. Their typical peak-to-peak timescales are 12–24 hr. Three of the bumps (*A*, *B*, and *C*) are of a similar structure during  $\sim 0.6$  days about their maximum. Later variations are harder to characterize because of the lower frequency of our sampling. Nonetheless, they seem to have a longer timescale. Periods of strong variability are still evident in the light curve tens of days after the burst.

We showed that the OT color changed during the first day after the burst. In the context of relativistic synchrotron models, this supports the suggestions, based on single-band light curves, that the ‘‘cooling-break’’ frequency passed through the optical bands around 0.25 days.

We discussed previous analysis of this event and found that the simple model involving a ‘‘jet break’’ occurring around day 0.5, proposed by several authors, is unable to account for the detailed optical data available for this event. At least two additional emission sources are required in order to sustain this interpretation: one to account for the flux observed from day 1 onward, as suggested by Berger et al. (2003), and another mechanism to account for the ubiquitous undulations detected in the light curves throughout the observed period, i.e., both before and after the jet break.

Examining an updated version of the Berger et al. (2003) model, we find that it provides a fair description of available multiband data. However, several discrepancies still need to be accounted for, probably requiring a self-consistent model for the mechanism producing the ubiquitous bumps and wiggles in the light curves of this event. A similar effort is required in order to test a simpler, empirically motivated singly broken power-law model we present.

A comprehensive effort to model the large volume of data collected for this burst, explicitly accounting for the variability on all timescales, seems to be the next challenge in making this unique event a key to understanding the GRB phenomenon. In this vein, in order to ensure the maximal usefulness of our observations to the community, we make all the data available through our Web site.<sup>14</sup>

We thank M. Uemura and R. A. Burenin for sending us a digital version of their light curves and Matheson et al. (2003) for the early release of their data to the community. We are grateful to A. Fruchter for sending us the host galaxy magnitude prior to publication. We acknowledge fruitful

<sup>14</sup> See <http://wise-obs.tau.ac.il/GRB030329>.

discussions with E. Waxman, D. Frail, and A. Levinson. Y. M. Lipkin and E. O. Ofek are grateful to the Dan-David prize foundation for financial support. A. Gal-Yam acknowledges a Colton Fellowship. Y. M. Lipkin, E. O. Ofek, A. Gal-Yam, D. Poznanski, and D. Polishook were supported in part by grants from the Israel Science Foundation. We thank

A. Henden and the USNO staff for providing us, and the GRB community in general, with field photometric calibration. We thank Eve Armstrong for observations at MDM, as well as the observers and staff of all the observatories that participated in this campaign, without which this work would not have been possible.

## REFERENCES

- Berezhiani, Z., Bombaci, I., Drago, A., Frontera, F., & Lavagno, A. 2003, *ApJ*, 586, 1250
- Berger, E., et al. 2000, *ApJ*, 545, 56
- . 2003, *Nature*, 426, 154
- Bersier, D., et al. 2003, *ApJ*, 584, L43
- Bloom, J. S., Djorgovski, S. G., Kulkarni, S. R., & Frail, D. A. 1998, *ApJ*, 507, L25
- Bloom, J. S., van Dokkum, P. G., Bailyn, C. D., Buxton, M. M., Kulkarni, S. R., & Schmidt, B. P. 2004, *AJ*, 127, 252
- Bloom, J. S., et al. 1999, *Nature*, 401, 453
- . 2002, *ApJ*, 572, L45
- Burenin, R. A., et al. 2003, *Astron. Lett.*, 29, 573
- Castro-Tirado, A. J., et al. 1999, *Science*, 283, 2069
- Chornock, R., Foley, R. J., Filippenko, A. V., Papankova, M., Weisz, D., & Garnavich, P. 2003, *IAU Circ.*, 8114, 2
- Dado, S., Dar, A., & De Rújula, A. 2003, *ApJ*, 594, L89
- Esin, A. A., & Blandford, R. 2000, *ApJ*, 534, L151
- Foley, R. J., et al. 2003, *PASP*, 115, 1220
- Fox, D. W., et al. 2003, *Nature*, 422, 284
- Frail, D. A., et al. 2001, *ApJ*, 562, L55
- Galama, T., et al. 1997, *Nature*, 387, 479
- Galama, T. J., Frail, D. A., Sari, R., Berger, E., Taylor, G. B., & Kulkarni, S. R. 2003, *ApJ*, 585, 899
- Galama, T. J., et al. 1998a, *Nature*, 395, 670
- . 1998b, *ApJ*, 497, L13
- Gal-Yam, A., Ofek, E. O., & Shemmer, O. 2002, *MNRAS*, 332, L73
- Garnavich, P., Stanek, K. Z., & Berlind, P. 2003a, *GRB Circ.*, 2018, 1
- Garnavich, P. M., Loeb, A., & Stanek, K. Z. 2000, *ApJ*, 544, L11
- Garnavich, P. M., et al. 2003b, *ApJ*, 582, 924
- Granot, J., Nakar, E., & Piran, T. 2003, *Nature*, 426, 138
- Greiner, J., Peimbert, M., Estaban, C., Kaufer, A., Jaunsen, A., Smoke, J., Klose, S., & Reimer, O. 2003a, *GRB Circ.*, 2020, 1
- Greiner, J., et al. 2003b, *Nature*, 426, 157
- Harrison, F. A., et al. 1999, *ApJ*, 523, L121
- Henden, A. 2003, *GRB Circ.*, 2082, 1
- Hjorth, J., et al. 2003, *Nature*, 423, 847
- Kawabata, K. S., et al. 2003, *ApJ*, 593, L19
- Kulkarni, S. R., et al. 1999, *Nature*, 398, 389
- Kumar, P., & Piran, T. 2000a, *ApJ*, 532, 286
- . 2000b, *ApJ*, 535, 152
- Lazzati, D., Rossi, E., Covino, S., Ghisellini, G., & Malesani, D. 2002, *A&A*, 396, L5
- Masetti, N., et al. 2000, *A&A*, 359, L23
- Matheson, T., et al. 2003, *ApJ*, 582, L5
- Mazzali, P. A., et al. 2003, *ApJ*, 599, L95
- McKenzie, E. H., & Schaefer, B. E. 1999, *PASP*, 111, 964
- Mirabal, N., et al. 2003, *ApJ*, 595, 935
- Nakar, E., Piran, T., & Granot, J. 2003, *NewA*, 8, 495
- Ofek, E. O., & Maoz, D. 2003, *ApJ*, 594, 101
- Panaitescu, A. 2001, *ApJ*, 556, 1002
- Panaitescu, A., Mészáros, P., & Rees, M. J. 1998, *ApJ*, 503, 314
- Pandey, S. B., Anupama, G. C., Sagar, R., Bhattacharya, D., Sahu, D. K., & Pandey, J. C. 2003, *MNRAS*, 340, 375
- Patat, F., et al. 2001, *ApJ*, 555, 900
- Perlmutter, S., et al. 1999, *ApJ*, 517, 565
- Peterson, B. A., & Price, P. A. 2003, *GRB Circ.*, 1985, 1
- Poznanski, D., Gal-Yam, A., Maoz, D., Filippenko, A. V., Leonard, D. C., & Matheson, T. 2002, *PASP*, 114, 833
- Price, P. A., et al. 2001, *ApJ*, 549, L7
- . 2003a, *ApJ*, 589, 838
- . 2003b, *Nature*, 423, 844
- Rees, M. J., & Mészáros, P. 1998, *ApJ*, 496, L1
- Reichart, D. E. 2001, *ApJ*, 554, 643
- Rhoads, J. E. 1997, *ApJ*, 487, L1
- Rhoads, J. E., & Fruchter, A. S. 2001, *ApJ*, 546, 117
- Sagar, R., Mohan, V., Pandey, S. B., Pandey, A. K., Stalin, C. S., & Castro Tirado, A. J. 2000, *Bull. Astron. Soc. India*, 28, 499
- Sari, R., Piran, T., & Halpern, J. P. 1999, *ApJ*, 519, L17
- Sari, R., Piran, T., & Narayan, R. 1998, *ApJ*, 497, L17
- Sato, R., et al. 2003, *ApJ*, 599, L9
- Schlegel, D. J., Finkbeiner, D. P., & Davis, M. 1998, *ApJ*, 500, 525
- Sheth, K., Frail, D. A., White, S., Das, M., Bertoldi, F., Walter, F., Kulkarni, S. R., & Berger, E. 2003, *ApJ*, 595, L33
- Smith, D. A., et al. 2003, *ApJ*, 596, L151
- Sokolov, V. V., Kopylov, A. I., Zharikov, S. V., Feroci, M., Nicastro, L., & Palazzi, E. 1998, *A&A*, 334, 117
- Stanek, K. Z., Garnavich, P. M., Kaluzny, J., Pych, W., & Thompson, I. 1999, *ApJ*, 522, L39
- Stanek, K. Z., et al. 2003, *ApJ*, 591, L17
- Stritzinger, M., et al. 2002, *AJ*, 124, 2100
- Tiengo, A., Mereghetti, S., Ghisellini, G., Rossi, E., Ghirlanda, G., & Schartel, N. 2003, *A&A*, 409, 983
- Torii, K. 2003, *GRB Circ.*, 1986, 1
- Torii, K., et al. 2003, *ApJ*, 597, L101
- Uemura, M., et al. 2003, *Nature*, 423, 843
- Urata, Y., et al. 2004, *ApJ*, 601, L17
- van Paradijs, J., et al. 1997, *Nature*, 386, 686
- Vanderspek, R., et al. 2003, *GRB Circ.*, 1997, 1
- Vietri, M., & Stella, L. 1998, *ApJ*, 507, L45
- Wang, X., & Loeb, A. 2000, *ApJ*, 535, 788
- Waxman, E., & Draine, B. T. 2000, *ApJ*, 537, 796
- Yokoo, T., Arimoto, J., Matsumoto, K., Takahashi, A., & Sadakane, K. 1994, *PASJ*, 46, L191
- Yoshii, Y., et al. 2003, *ApJ*, 592, 467
- Zeh, A., Klose, S., & Hartmann, D. H. 2003, *ApJ*, submitted (astro-ph/0311610)